

Comparison of the Particle Flow in $q\bar{q}g$ and $q\bar{q}\gamma$ Events in e^+e^- Annihilation

H. Aihara, M. Alston-Garnjost, R. E. Avery, A. Barbaro-Galtieri, A. R. Barker, A. V. Barnes, B. A. Barnett, D. A. Bauer, H.-U. Bengtsson, D. L. Bintinger, G. J. Bobbink, T. S. Bolognese, A. D. Bross, C. D. Buchanan, A. Buijs, M. P. Cain, D. O. Caldwell, A. R. Clark, G. D. Cowan, D. A. Crane, O. I. Dahl, K. A. Derby, J. J. Eastman, P. H. Eberhard, A. M. Eisner, R. Enomoto, F. C. Ern e, T. Fujii, J. W. Gary, W. Gorn, J. M. Hauptman, W. Hofmann, J. E. Huth, J. Hylen, T. Kamae, H. S. Kaye, K. H. Kees, R. W. Kenney, L. T. Kerth, Winston Ko, R. I. Koda, R. R. Kofler, K. K. Kwong, R. L. Lander, W. G. J. Langeveld, J. G. Layter, F. L. Linde, C. S. Lindsey, S. C. Loken, A. Lu, X.-Q. Lu, G. R. Lynch, R. J. Madaras, K. Maeshima, B. D. Magnuson, J. N. Marx, K. Maruyama, G. E. Masek, L. G. Mathis, J. A. J. Matthews, S. J. Maxfield, S. O. Melnikoff, E. S. Miller, W. Moses, R. R. McNeil, P. Nemethy, D. R. Nygren, P. J. Oddone, H. P. Paar, D. A. Park, D. E. Pellet, M. Pripstein, M. T. Ronan, R. R. Ross, F. R. Rouse, K. A. Schwitkis, J. C. Sens, G. Shapiro, M. D. Shapiro, B. C. Shen, W. E. Slater, J. R. Smith, J. S. Steinman, M. L. Stevenson, D. H. Stork, M. G. Strauss, M. K. Sullivan, T. Takahashi, J. R. Thompson, N. Toge, R. van Tyen, B. van Uiter, G. J. VanDalen, R. R. van Daalen Wetters, W. Vernon, W. Wagner, E. M. Wang, Y. X. Wang, M. R. Wayne, W. A. Wenzel, J. T. White, M. S. C. Williams, Z. R. Wolf, H. Yamamoto, M. Yamauchi, S. J. Yellin, C. Zeitlin, and W.-M. Zhang

(TPC/Two-Gamma Collaboration)

Lawrence Berkeley Laboratory, Berkeley, California 94720

University of California, Davis, Davis, California 95616

University of California Institute for Research at Particle Accelerators, Stanford, California 94305

University of California, Los Angeles, Los Angeles, California 90024

University of California, Riverside, Riverside, California 92521

University of California, San Diego, La Jolla, California 92093

University of California, Santa Barbara, Santa Barbara, California 93106

Carnegie-Mellon University, Pittsburgh, Pennsylvania 15213

Ames Laboratory, Iowa State University, Ames, Iowa 50011

John Hopkins University, Baltimore, Maryland 21218

University of Massachusetts, Amherst, Massachusetts 01003

New York University, New York, New York 10003

National Institute for Nuclear and High Energy Physics, Amsterdam, The Netherlands

University of Tokyo, Tokyo, Japan

(Received 30 June 1986)

We compare the particle flow in the event plane of three-jet $q\bar{q}g$ (quark-antiquark-gluon) events with the particle flow in radiative annihilation events $q\bar{q}\gamma$ (quark-antiquark-photon) for similar kinematic configurations. In the angular region between quark and antiquark jet, we find a significant decrease in particle density for $q\bar{q}g$ as compared to $q\bar{q}\gamma$. This effect is predicted in QCD as a result of destructive interference between soft-gluon radiation from quark, antiquark, and hard gluon.

PACS numbers: 13.65.+i, 12.38.Qk

The study of the particle flow in three-jet ($q\bar{q}g$) events from e^+e^- annihilation has proven a powerful tool to disentangle the global structure of the process of quark and gluon hadronization.^{1,2} Here, we present a test of recent QCD predictions concerning the azimuthal distribution of hadrons in the event plane of events with a large-angle gluon jet. The (infrared-safe) predictions³ are based on the hypothesis of local parton-hadron duality which assumes that the angular distribution of soft hadrons closely reflects the flow of soft gluons emitted from the primary "color antenna,"

namely the color sources created in the initial hard subprocess: q , \bar{q} , and g . The calculations predict a particular effect in three-jet events (see Fig. 1): In the azimuthal region between q and \bar{q} (i.e., opposite to the gluon jet), negative interference between radiation from the gluon and radiation from quark and antiquark results in a sizable reduction of soft-gluon and, hence, particle density. The effect can be tested by comparison of $q\bar{q}g$ three-jet events with events where the gluon is replaced by a radiative photon with otherwise identical kinematics. In the latter events, the negative

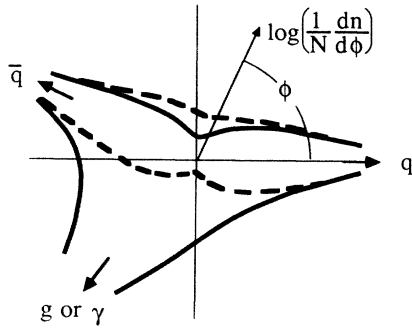


FIG. 1. Directivity diagram of soft-gluon flow in $q\bar{q}g$ (solid) and $q\bar{q}\gamma$ (dashed) events, projected into event planes defined by the q and \bar{q} momentum vectors. The distance from the origin represents the density $(1/N_{\text{event}})(dn_{\text{gluon}}/d\phi)$ of soft gluons emitted at an azimuthal angle ϕ with respect to the quark jet. Note that the radial scale is logarithmic; the normalization is arbitrary, but identical for $q\bar{q}g$ and $q\bar{q}\gamma$. From Ref. 3.

interference is missing, thereby increasing the prediction for the particle density in the region between q and \bar{q} by about a factor 2 relative to $q\bar{q}g$ events.³ In this Letter, we present a first comparison of the particle flow in $q\bar{q}g$ and $q\bar{q}\gamma$ events.

The data were recorded with the TPC facility at the SLAC e^+e^- storage ring PEP operating at 29-GeV c.m.-system energy. The time projection chamber⁴ (TPC) was used to track charged particles with $p > 0.15$ GeV over 87% of 4π ; the hexagonal calorimeter⁵ (HEX) detected photons with $E > 0.4$ GeV over 70% of 4π . Data were taken with two different detector configurations: a first sample of 77 pb^{-1} with the TPC operating in the 4-kG field of a normal solenoid, and a more recent sample of about 70 pb^{-1} with a 13.25-kG superconducting coil. As a result of the higher field and the addition of a gating system to reduce space-charge-induced distortions in the TPC, the momentum resolution improved from $[(3.5 \text{ GeV}^{-1})p]\%$ for the first data set to $[(0.6 \text{ GeV}^{-1})p]\%$ for the second sample. The HEX achieves a typical resolution of $[(17 \text{ GeV}^{1/2})E^{-1/2}]\%$ for energies below 1 GeV, and a nearly constant resolution above.

Three different event types were selected for this analysis: three-jet events (" $q\bar{q}g$ "), two-jet events with a radiative photon detected in the HEX (" $q\bar{q}\gamma$ "), and noncollinear two-jet events with a radiative photon escaping down the beam line (" $q\bar{q}[\gamma]$ "). The two different samples of radiative events have completely different systematics and provide an excellent cross check. To select the events, the eigenvalues $Q_1 > Q_2 > Q_3$ of the sphericity tensor were calculated. A jet-finding algorithm² was applied to planar ($Q_3 < 0.06$) events. Those events with $Q_2 - Q_3$

> 0.05 and with three reconstructed jets were considered $q\bar{q}g$ candidates; their event plane was defined by the eigenvectors of the sphericity tensor corresponding to Q_1 and Q_2 . Events with $Q_3 < 0.06$ and two noncollinear jets supplied the $q\bar{q}[\gamma]$ candidates; here an event plane was defined by the e^+e^- beam line (z) and the largest eigenvector of a "sphericity" tensor calculated from only momentum components (x, y) perpendicular to the beam line. Finally, planar events with an isolated energy deposition in the HEX of at least 3.5 GeV were counted as $q\bar{q}\gamma$ candidates. The energy deposition must not be associated with a charged track, and the scalar sum of charged- plus neutral-particle momenta within a 30° cone around the HEX hit must not exceed 0.5 GeV. We refer to the HEX hit as a photon, although there is a chance that a high-energy π^0 fakes an isolated hit. As for the three-jet case, an event plane is assigned based on eigenvectors of the sphericity tensor. Particles are assigned to two jets by boosting of the hadronic system into its rest frame (derived from the measured photon momentum) and by division of particles into those moving forward and backward with respect to the sphericity axis in this system (calculated under exclusion of the high-momentum photon). Furthermore, a minimum angle of 25° between sphericity axis and photon is required. In all cases, final jet directions are defined by the momentum sums of charged and neutral particles assigned to a jet.

Parton or photon energies E_1, E_2, E_3 were calculated from the jet or photon directions (projected into the event plane), with neglect of jet masses. For $q\bar{q}[\gamma]$ candidates the beam axis was assumed for the photon direction. The jets (for simplicity, we refer in the following to the photon as a "jet") are enumerated such that $E_1 > E_2 > E_3$. In the $q\bar{q}g$ sample, jet 3 is assumed to be the gluon; in the $q\bar{q}\gamma$ and $q\bar{q}[\gamma]$ samples, the photon is required to be the lowest-energy jet. In either case, jets 1 and 2 must have a scalar sum of particle momenta exceeding 2.5 GeV, and must contain at least 3 particles. The scalar sum of particle momenta in jets 1 and 2 together must exceed half the beam energy, or 7.25 GeV. To reject τ events, at least one of the jets 1,2 must have a mass > 2 GeV or more than 3 charged particles. Jet 3 of $q\bar{q}g$ candidates must consist of at least 3 particles with a scalar momentum sum in excess of 1.5 GeV, and less than 6 GeV. In all cases, we use only events with $4 < E_3 < 9$ GeV. The three jets have to be coplanar within 20° (10° for $q\bar{q}[\gamma]$); jets 1 and 2 must deviate from collinearity by at least 3 standard deviations (calculated with use of energy-dependent angular errors on the jet axes derived from a Monte Carlo simulation). For the $q\bar{q}\gamma$ events, a (loose) match between measured and calculated photon energy is required. In order to ensure similar experimental acceptances for $q\bar{q}g$ and $q\bar{q}\gamma$ events, the

TABLE I. Summary of properties of $q\bar{q}g$, $q\bar{q}\gamma$, and $q\bar{q}[\gamma]$ event samples.

	$q\bar{q}g$	$q\bar{q}\gamma$	$q\bar{q}[\gamma]$
Number of events	2537	117	1564
Number/(expected number) ^a	1.00 ± 0.05	0.99 ± 0.14	0.98 ± 0.06
$\langle E_1 \rangle$ (GeV)	12.7	12.7	12.2
$\langle E_2 \rangle$ (GeV)	10.2	10.0	9.9
$\langle E_3 \rangle$ (GeV)	6.1	6.3	6.9
$\langle \phi_1 \rangle$	$\equiv 0$	$\equiv 0$	$\equiv 0$
$\langle \phi_2 \rangle$ (deg)	153	152	145
$\langle \phi_3 \rangle$ (deg)	231	229	235

^aIncludes systematic errors in the acceptance calculations. The expected number of $q\bar{q}g$ events is based on the α_s value determined from a global fit to the data (Ref. 2). The expected numbers for radiative events include (small) corrections for final-state radiation from quarks (Ref. 7).

gluon jet in $q\bar{q}g$ is required to point towards the HEX; furthermore, the angle between the sphericity axis of a $q\bar{q}g$ or $q\bar{q}\gamma$ event and the beam line must exceed 45° .

On the basis of Monte Carlo simulations using the LUND event generator⁶ and a detailed modeling of the detector, we expect that the event type is correctly identified as $q\bar{q}g$ (with the gluon as jet 3), $q\bar{q}\gamma$, or $q\bar{q}[\gamma]$ in approximately 60%, 75%, and 70% of the events, respectively. Contamination of the samples from τ pairs, QED, and two-photon events is negligible (below 2%). The data presented below are corrected for detector acceptance. No attempt has been made to unfold possible misclassification of event types or jets. Since the low- and high-field data samples proved consistent with statistical errors, the two data sets were merged after separate acceptance corrections.

Sample sizes and main characteristics of the $q\bar{q}g$, $q\bar{q}\gamma$, and $q\bar{q}[\gamma]$ events are summarized in Table I. Within errors the $q\bar{q}\gamma$, $q\bar{q}[\gamma]$, and $q\bar{q}g$ event rates agree with expectations from QED and QCD, respectively. For jets and particles, the azimuthal angle ϕ in the event plane is measured with respect to the highest-momentum jet (1); the events are oriented such that jet 2 falls into the second quadrant. For the three classes of events, energies $E_{1,2,3}$ and angles $\phi_{1,2,3}$ of the jets are similar, allowing a direct comparison of the event structure.

The flow of charged hadrons $(1/N_{\text{event}})(dn/d\phi)$ as a function of the azimuthal angle ϕ in the event plane ("directivity diagram") is shown in Fig. 2(a), for both the $q\bar{q}g$ and $q\bar{q}\gamma$ events. An excess of particle production is apparent in the region between jets 1 and 2 of $q\bar{q}\gamma$ events, as compared to $q\bar{q}g$ events. This is exactly the effect predicted by the QCD modeling—a negative interference of gluon radiation opposite to the gluon jet (3) in $q\bar{q}g$ events. Also shown in Fig. 2(a) are QCD predictions for asymptotic energies³ for the flow of soft gluons in $q\bar{q}g$ events (solid line; jet 3 is assumed to be the gluon) and $q\bar{q}\gamma$ events (dashed). In its range of validity (not too close to the parton directions) the predicted shape agrees rather well with the

measured distribution for hadrons, except in the region around the gluon jet. Here asymptotic QCD predicts a ratio 9/4 for soft-gluon multiplicities in

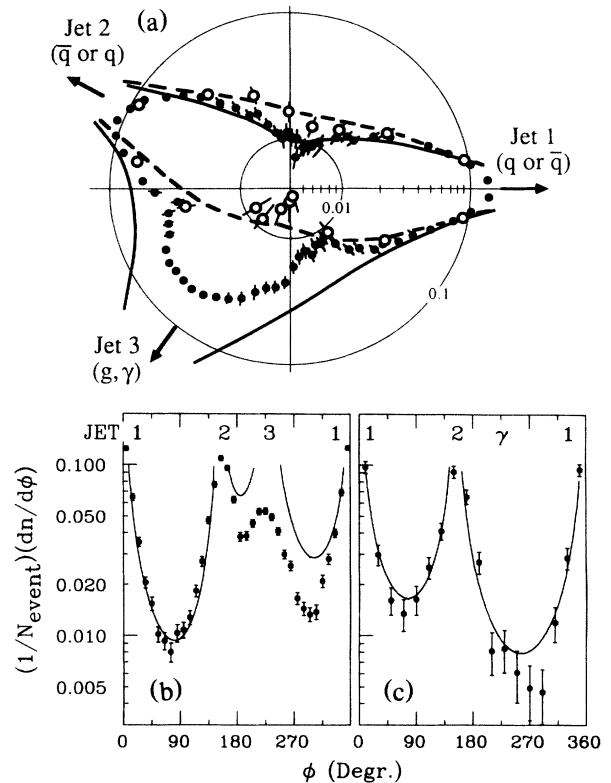


FIG. 2. (a) Directivity diagram of charged-hadron flow in the event plane, $(1/N_{\text{event}})(dn/d\phi)$, as a function of the azimuthal angle ϕ , for $q\bar{q}g$ events (solid circles) and $q\bar{q}\gamma$ events (open circles). In $q\bar{q}g$ events, jet 3 is typically the gluon, whereas jet 1 and jet 2 are q or \bar{q} jets. Solid lines, asymptotic QCD predictions for the flow of soft gluons (Ref. 3), for $\phi_q = 0$, $\phi_{\bar{q}} = 153^\circ$, $\phi_{g,\gamma} = 231^\circ$; the normalization is arbitrary, but identical for $q\bar{q}g$ (solid) and $q\bar{q}\gamma$ (dashed). Radial scale is logarithmic. (b), (c) Alternative presentation of the (b) $q\bar{q}g$ and (c) $q\bar{q}\gamma$ data. Full lines represent QCD predictions.

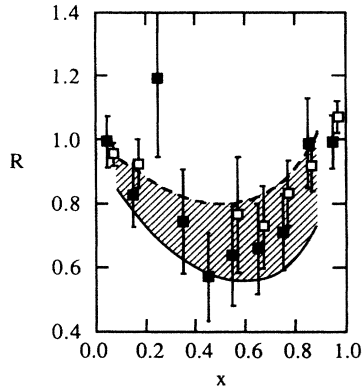


FIG. 3. Solid squares, ratio R of the particle flow in $q\bar{q}g$ and in $q\bar{q}\gamma$ events, in the region between jets 1 and 2, as a function of the scaled angle $x = \phi/\phi_{12}$. Open squares, ratio R of the particle flow in $q\bar{q}g$ and in $q\bar{q}[\gamma]$ events. Shaded area, range of (asymptotic) QCD predictions (Ref. 3); see text for details.

hard-gluon and quark jets (compared to typical ratios for hadron multiplicities around 1.3 at our energies,⁸ where pre-asymptotic effects are of importance) and the particle density is overestimated. An alternative presentation of data and QCD predictions is given in Figs. 2(b) and 2(c).

In order to simplify the comparison and to reduce the effect of the slight difference in opening angle ϕ_{12} between jets 1 and 2 for the three event samples, we calculate the flow of charged hadrons in the 1-2 region as a function of the normalized angle $x = \phi/\phi_{12}$. The ratio

$$R = \frac{(1/N_{q\bar{q}g})(dn/dx)_{q\bar{q}g}}{(1/N_{q\bar{q}\gamma})(dn/dx)_{q\bar{q}\gamma}}$$

is displayed in Fig. 3 (full squares), and clearly deviates from unity ($N_{q\bar{q}g}$ and $N_{q\bar{q}\gamma}$ stand for the number of $q\bar{q}g$ and $q\bar{q}\gamma$ events, respectively).

Unlike the $q\bar{q}g$ and $q\bar{q}\gamma$ events, the $q\bar{q}[\gamma]$ events suffer from the problem that the event plane contains the beam line (by definition); some of the particles in the interesting region between jets 1 and 2 are inevitably lost in the forward holes of the detector system. Using only the x or ϕ regions fully covered by the detector acceptance (open squares in Fig. 3), we find good agreement between the $q\bar{q}\gamma$ and $q\bar{q}[\gamma]$ event samples.

Included in Fig. 3 are (asymptotic) QCD predictions³ for the ratio of the flow of soft gluons in $q\bar{q}g$ and $q\bar{q}\gamma$ events. The full line gives the prediction for the case that the gluon jet is always correctly identified as jet 3, whereas the dashed line represents an attempt to account for misidentification of gluon jet. Since the

asymptotic QCD calculation overpredicts the particle multiplicity in hard-gluon jets (see above), the increase in R due to jet 1 or 2 being the gluon is most likely overestimated. The data fall roughly in between the two curves.

In order to demonstrate that the observed deviation of R from unity is not due to selection biases, we generated predictions from an independent-fragmentation Monte Carlo event generator,⁶ where each parton fragments independently in the overall $q\bar{q}g$ or $q\bar{q}\gamma$ center-of-mass system. Such a model is equivalent to a QCD calculation where the interference of radiation from different color sources is neglected.³ The independent-fragmentation prediction for R is consistent with unity (within ± 0.07) and is incompatible with the data.

In summary, we have shown that the flow of soft hadrons into the angular region between q and \bar{q} jets in $q\bar{q}g$ events is reduced compared to that in $q\bar{q}\gamma$ events, in agreement with QCD predictions and in support of the concept of local parton-hadron duality. The observed effect is, of course, equivalent to the "string effect"^{1,2}—indeed it can be shown³ that the particle flow in the string model approximates the QCD result rather well, up to terms of order $1/N_c$. However, the comparison of $q\bar{q}g$ and $q\bar{q}\gamma$ events allows for the first time a model-independent measurement of this phenomenon.

We acknowledge the efforts of the PEP staff, and the engineers, programmers, and technicians who made this work possible. This work was supported by the U.S. Department of Energy under Contracts No. DE-AC03-76SF00098, No. DE-AM03-76SF00034, and No. DE-AC02-76ER03330, by the National Science Foundation, and by the Joint Japan-U.S. Collaboration in High Energy Physics, One of us (W.H.) acknowledges receipt of an A.P. Sloan Fellowship.

¹W. Bartel *et al.*, *Z. Phys. C* **21**, 37 (1983), and *Phys. Lett.* **134B**, 275 (1984), and **157B**, 340 (1985); M. Althoff *et al.*, *Z. Phys. C* **29**, 29 (1985).

²H. Aihara *et al.*, *Z. Phys. C* **28**, 31 (1985).

³Ya. I. Azimov, Yu. L. Dokshitzer, V. A. Khoze, and S. I. Troyan, *Phys. Lett.* **165B**, 147 (1985).

⁴H. Aihara *et al.*, *Phys. Rev. Lett.* **52**, 577 (1984).

⁵H. Aihara *et al.*, *Nucl. Instrum. Methods* **217**, 259 (1983).

⁶T. Sjöstrand, *Comput. Phys. Commun.* **27**, 243 (1982); and **28**, 229 (1983). We used version 5.3 of the event generator. For the independent-fragmentation modeling of $q\bar{q}\gamma$ events, the generator was modified such as to fragment partons independently in the overall ($q\bar{q}\gamma$) c.m.-system frame.

⁷E. Laermann, T. F. Walsh, I. Schmitt, and P. M. Zerwas, *Nucl. Phys.* **B207**, 205 (1982).

⁸M. Derrick *et al.*, *Phys. Lett.* **165B**, 449 (1985).